Hybrid quantum scattering algorithms for longrange potentials

Millard H. Alexander

Citation: The Journal of Chemical Physics **81**, 4510 (1984); doi: 10.1063/1.447420
View online: http://dx.doi.org/10.1063/1.447420
View Table of Contents: http://scitation.aip.org/content/aip/journal/jcp/81/10?ver=pdfcov
Published by the AIP Publishing

Hybrid quantum scattering algorithms for long-range potentials

Millard H. Alexander
Department of Chemistry, University of Maryland, College Park, Maryland 20742

(Received 9 May 1984; accepted 3 July 1984)

We investigate hybrid scattering codes which combine the log-derivative integrator (LOGD) of Johnson at short range with one of the three following integrators at moderate to long range: the multichannel WKB algorithm of Johnson, the variable-interval-variable-step (VIVS) algorithm of Parker, Schmalz, and Light, or a new algorithm (AIRY) based on the linear reference potential algorithm of Gordon modified to propagate the log-derivative matrix directly without determination of perturbation corrections. In calculations of S matrices for the collision of two HF molecules, where the off-diagonal coupling decreases only as R^{-3}, the AIRY integrator is found to be 3 times faster than the WKB integrator, at least 5 times faster than the VIVS integrator, and 19 times faster than direct application of the LOGD integrator in the long-range region.

I. INTRODUCTION

There has been considerable past interest in the development of efficient algorithms and computer codes for the solution of the close-coupling (CC) equations which arise in the quantum description of inelastic atomic and molecular collisions.[1] A major conclusion[2] of a workshop run by the National Resource for Computation in Chemistry (NRCC)[3,4] was that hybrid integration algorithms are the most efficient. At short range, where the potential is rapidly varying, a "solution-following" algorithm[1] is preferable, to be replaced by a "potential following" algorithm[1] at longer range when the potential is slowly varying compared to the local deBroglie wavelength of the collision partners. This NRCC workshop recommended[2,4] the log-derivative (LOGD) algorithm of Johnson[5-7] at short range and the variable-interval-variable-step (VIVS) algorithm of Parker, Schmalz, and Light[8] at long range. A generalized scattering code, named VIVAS, which incorporates these two integrators, has been written.[9]

Over the past decade we[10-12] and others[13] have been engaged in quantum studies of collisions of polar molecules, where the potential matrix elements decay asymptotically only as the third power of the intermolecular separation. A similar asymptotic dependence characterizes the van der Waals interaction of atoms or molecules with surfaces.[14,15] Because of the importance of these systems it is desirable to develop hybrid scattering codes which are particularly efficient for R^{-3} potentials. This is the goal of the work reported here.

We have investigated three different integrators for the long-range region: The VIVS algorithm,[8] a multichannel WKB method developed by Johnson,[16] and a variation of the original Gordon algorithm,[17,18] designed to propagate directly the log-derivative matrix. These three integrators were tested, both for accuracy and speed, on a typical long-range collision system, namely the collision of two HF molecules. In all cases the original LOGD algorithm[5-7] was used for the short-range region.

The organization of this article is as follows: the next section reviews the general structure of the CC equations and the LOGD algorithm. In Sec. III the three long-range integrators are described. The actual numerical tests are summarized in Sec. IV. A brief conclusion follows.

II. CLOSE COUPLING EQUATIONS

Using as closely as possible the same notation as Secrest[1] in his review article, we write the CC equations as

$$\left[-\frac{d^2}{dR^2}+\frac{l_i(l_i+1)}{R^2}-k_i^2\right]F_{iI}=-\sum_{i'}V_{ii'}(R)F_{i'I}(r), \tag{1}$$

where l_i and k_i designate, respectively, the orbital angular momentum and wave vector in the ith channel. Equivalently, Eq. (1) can be written in matrix notation as

$$\left[\mathbf{I}\frac{d^2}{dR^2}+\mathbf{W}(R)\right]\mathbf{F}(R)=0, \tag{2}$$

where $\mathbf{I}$ is the identity matrix, and

$$\mathbf{W}(R)=\mathbf{k}^2-\mathbf{l}^2(R)/R^2-\mathbf{V}(R), \tag{3}$$

with $\mathbf{k}^2$ and $\mathbf{l}^2$ being diagonal matrices.

The LOGD algorithm of Johnson[5-7] propagates the logarithmic derivative of $\mathbf{F}$, namely

$$\mathbf{Y}(R)=\mathbf{F}'(R)\mathbf{F}(R)^{-1}. \tag{4}$$

The matrix $\mathbf{Y}(R)$ is propagated numerically in terms of a matrix $\mathbf{Z}_n=h\mathbf{Y}_n$, where h designates the interval size ($h=R_{n+1}-R_n$). An inversion of the $\mathbf{Z}$ matrix is required at every interval, and, at every other interval, an additional inversion of the matrix $[\mathbf{I}+(h^2/6)\mathbf{W}(R)]$,[6,7] resulting in a total of 1.5 matrix inversions per interval.

Whenever the channel wavevectors are large, the interval size is small, or the off-diagonal elements of $\mathbf{V}(R)$ are small, the following simple approximation can be used to perform this latter matrix inversion:

$$[A^{-1}]_{ii}\simeq 1/A_{ii}, \tag{5a}$$

$$[A^{-1}]_{i,j\neq i}\simeq -A_{ij}/A_{ii}A_{jj}, \tag{5b}$$

which becomes increasingly accurate as the diagonal elements of $\mathbf{A}$ become large compared with the off-diagonal elements. Since implementation of Eq. (5) requires only M^2 operations, where M is the order of the matrix, rather than M^3 for a conventional matrix inversion, in some cases the

 0021-9606/84/224510-07$02.10

overhead of the LOGD algorithm can be reduced to only one matrix inversion per interval.

In the hybrid scattering codes to be discussed below the LOGD algorithm is used to propagate the **Z** matrix starting at a point $R_0 \equiv R_{\rm start}$, lying well within the classically forbidden region, to some larger value of R which we designate $R_{\rm begin} \equiv R_N$, at which point a switch is made to an integrator more appropriate to the large-R region, where the potential is slowly varying.

The actual codes used in the numerical tests to be described in Sec. IV incorporated the original LOGD code of Johnson,[19] modified to allow this faster approximate matrix inversion [Eq. (5)] whenever appropriate.

III. LONG-RANGE INTEGRATORS

A. AIRY algorithm

The ending point of the LOGD integration, $R_{\rm begin}$, will be chosen so that for $R > R_{\rm begin}$, $\mathbf{W}(R)$ will be slowly varying on the scale of the local deBroglie wavelength of the individual channel wave functions. In this region we shift to a locally adiabatic approximation. In the nth interval in this large-R region we define an orthogonal transformation $\mathbf{T}_n$, chosen to diagonalize $\mathbf{W}(R)$ at the midpoint ($R = R_{n+1/2}$) of the interval. We have

$$\mathbf{T}_n \mathbf{W}(R_{n+1/2}) \mathbf{T}_n^T = \tilde{\mathbf{k}}_n^2, \tag{6}$$

where $\tilde{\mathbf{k}}_n^2$ is a diagonal matrix. In the so-called "local basis"[17,18] the solution matrix becomes

$$\tilde{\mathbf{F}}_n = \mathbf{T}_n \mathbf{F}_n. \tag{7}$$

One can show[1,17,18] that $\tilde{\mathbf{F}}_n$ satisfies the following equation:

$$[\mathbf{I} d^2/dR^2 + \tilde{\mathbf{k}}_n^2 + \tilde{\mathbf{W}}_n'(R - R_{n+1/2}) + \tilde{\mathbf{W}}_n''(R - R_{n+1/2})^2 + \cdots] \tilde{\mathbf{F}}_n = 0, \tag{8}$$

where

$$\tilde{\mathbf{W}}_n' = \mathbf{T}_n (d\mathbf{W}/dR)_{R_{n+1/2}} \mathbf{T}_n^T \tag{9}$$

and

$$\tilde{\mathbf{W}}_n'' = \tfrac{1}{2} \mathbf{T}_n (d^2\mathbf{W}/dR^2)_{R_{n+1/2}} \mathbf{T}_n^T. \tag{10}$$

Propagation across the nth interval (from R_n to R_{n+1}) is formally equivalent to defining a procedure whereby the solution matrix $\tilde{\mathbf{F}}_n$ and its first derivative $\tilde{\mathbf{F}}_n'$ at $R = R_{n+1}$ can be obtained in terms of their values at $R = R_n$. For a second-order differential equation one can write[7,18,20]

$$\tilde{\mathbf{F}}_n(R_{n+1}) = \mathbf{A}_n \tilde{\mathbf{F}}_n(R_n) + \mathbf{B}_n \tilde{\mathbf{F}}_n'(R_n) \tag{11}$$

and

$$\tilde{\mathbf{F}}_n'(R_{n+1}) = \mathbf{C}_n \tilde{\mathbf{F}}_n(R_n) + \mathbf{D}_n \tilde{\mathbf{F}}_n'(R_n), \tag{12}$$

where $\mathbf{A}_n$, $\mathbf{B}_n$, $\mathbf{C}_n$, and $\mathbf{D}_n$ are square matrices of order equal to the number of channels. If we define the log-derivative matrix in the local basis $\tilde{\mathbf{Y}}_n$ similarly to Eq. (4), then one can show that Eqs. (11) and (12) lead to an equivalent equation for the propagation of this matrix, namely

$$\tilde{\mathbf{Y}}_n(R_{n+1}) = [\mathbf{C}_n + \mathbf{D}_n \tilde{\mathbf{Y}}_n(R_n)] [\mathbf{A}_n + \mathbf{B}_n \tilde{\mathbf{Y}}_n(R_n)]^{-1}. \tag{13}$$

Light and co-workers[20] have derived similar relations for propagation of the so-called **R** matrix, which is the inverse of the log-derivative matrix. In exploring the connection between Eqs. (11)–(13) and this earlier work, the reader should observe that there the derivatives are defined in the *outward* rather than *positive* sense, so that the $\tilde{\mathbf{F}}_n'(R_n)$ of Light and co-workers[20] is the *negative* of the quantity which appears in Eqs. (11) and (12).

If the off-diagonal elements of the $\tilde{\mathbf{W}}_n'$, $\tilde{\mathbf{W}}_n''$ (and higher derivative) matrices are neglected, then the $\mathbf{A}_n$, $\mathbf{B}_n$, $\mathbf{C}_n$, and $\mathbf{D}_n$ matrices in Eqs. (11)–(13) are diagonal, with elements which can be expressed in terms of the two linearly independent solutions to an ordinary second-order differential equation, the so-called "reference" equation, namely[1,8,17,18]

$$[d^2/dR^2 + (\tilde{k}_n^2)_{ii} + (\tilde{W}_n')_{ii}(R - R_{n+1/2}) + (\tilde{W}_n'')_{ii}(R - R_{n+1/2})^2 + \cdots] \begin{matrix} f_i^{(n)}(R) \\ g_i^{(n)}(R) \end{matrix} = 0. \tag{14}$$

One has[18,20]

$$(A_n)_{ij} = \delta_{ij} [f_i^{(n)}(R_{n+1}) g_i^{(n)\prime}(R_n) - g_i^{(n)}(R_{n+1}) f_i^{(n)\prime}(R_n)]/w_i, \tag{15}$$

$$(B_n)_{ij} = \delta_{ij} [g_i^{(n)}(R_{n+1}) f_i^{(n)}(R_n) - f_i^{(n)}(R_{n+1}) g_i^{(n)}(R_n)]/w_i, \tag{16}$$

$$(C_n)_{ij} = \delta_{ij} [f_i^{(n)\prime}(R_{n+1}) g_i^{(n)\prime}(R_n) - g_i^{(n)\prime}(R_{n+1}) f_i^{(n)\prime}(R_n)]/w_i, \tag{17}$$

and

$$(D_n)_{ij} = \delta_{ij} [g_i^{(n)\prime}(R_{n+1}) f_i^{(n)}(R_n) - f_i^{(n)\prime}(R_{n+1}) g_i^{(n)}(R_n)]/w_i, \tag{18}$$

where w_i denotes the R-independent Wronskian of the two solutions

$$w_i = f_i^{(n)}(R) g_i^{(n)\prime}(R) - f_i^{(n)\prime}(R) g_i^{(n)}(R). \tag{19}$$

Since $\mathbf{A}_n$, $\mathbf{B}_n$, $\mathbf{C}_n$, and $\mathbf{D}_n$ are diagonal, one can show that the propagation defined by Eq. (13) preserves the symmetry of the log-derivative matrix, which allows us to obtain the log-derivative matrix at R_{n+1} in terms of its value at R_n by solution of the following set of linear equations:

$$[\mathbf{a}_n + \tilde{\mathbf{Y}}_n(R_n) \mathbf{b}_n] \tilde{\mathbf{Y}}_n(R_{n+1}) = \mathbf{c}_n + \tilde{\mathbf{Y}}_n(R_n) \mathbf{d}_n, \tag{20}$$

where lower-case letters are used to indicate explicitly the diagonal character of the matrices defined by Eqs. (15)–(18).

As discussed originally by Gordon,[17] the local solution matrix at the left-hand side of the nth interval can be related to the solution matrix at the right-hand side of the $(n-1)$th interval by

$$\tilde{\mathbf{F}}_n(R_n) = \mathbf{P}_n \tilde{\mathbf{F}}_{n-1}(R_n), \tag{21}$$

where

$$\mathbf{P}_n = \mathbf{T}_n \mathbf{T}_{n-1}^T. \tag{22}$$

Since a similar relation applies to the first derivative of $\tilde{\mathbf{F}}_n$, it follows that passage from one locally adiabatic basis to the next necessitates the following transformation of the log-derivative matrix[21]:

$$\tilde{\mathbf{Y}}_n(R_n) = \mathbf{P}_n \tilde{\mathbf{Y}}_{n-1}(R_n) \mathbf{P}_n^T, \tag{23}$$

which is an orthogonal transformation, since $\mathbf{P}_n^{-1} = \mathbf{P}_n^T$.

In our hybrid code the value of the local log-derivative matrix at the left-hand side of the first interval is obtained from the value at $R = R_{\rm begin}$, obtained by integration from $R = R_{\rm start}$ to $R = R_{\rm begin}$ using the LOGD algorithm (Sec.

II). Since for $R < R_{\text{begin}}$ the Schrodinger equation is formulated in the asymptotic basis, $\mathbf{P}_1 = \mathbf{T}_1$ in Eq. (23) for $n = 1$. Repeated application of Eqs. (20) and (23) allows propagation of the solution from R_{begin} to R_{end}, by which point the potential has become vanishingly small. To obtain an S matrix it is necessary to transform the log-derivative matrix back into the asymptotic basis at the right-hand side of the last (Nth) interval, so that

$$\mathbf{Y}(R = R_{\text{end}}) = \mathbf{T}_N^T \tilde{\mathbf{Y}}_N(R = R_{N+1} = R_{\text{end}})\mathbf{T}_N. \tag{24}$$

Gordon has shown[17] how if the first derivative terms in Eq. (14) are retained, but higher derivatives are neglected, the solutions to Eq. (14) are Airy functions. The diagonal matrix elements of the $\mathbf{A}_n$, $\mathbf{B}_n$, $\mathbf{C}_n$, and $\mathbf{D}_n$ matrices [Eqs. (15)–(18)] can be obtained directly from the subroutine SPROP of Gordon's original code.[22] Gordon has discussed[18] how these coefficients can be calculated with much greater numerical stability than the individual Airy functions themselves.

It is possible to determine, at least approximately, the corrections to the $\mathbf{A}_n$, $\mathbf{B}_n$, $\mathbf{C}_n$, and $\mathbf{D}_n$ matrices resulting from the neglected elements of the $\tilde{\mathbf{W}}_n''$ matrix [Eq. (10)] and from the neglected off-diagonal elements of the $\tilde{\mathbf{W}}_n'$ matrix [Eq. (9)].[17,18] This greatly increases the complexity of the resulting code and, as will be seen in Sec. IV, does not appear to be desirable, at least for the present application.

A crucial element in the application of any locally adiabatic method is the algorithm for choosing the interval sizes. In the original Gordon code,[22] and in the VIVAS code to be discussed below,[23] this is done by examination of the magnitude of the correction terms mentioned in the preceding paragraph. We have devised an alternative, simple algorithm based on the crudest estimate of these correction terms. For the neglected off-diagonal elements of the $\tilde{\mathbf{W}}_n'$ matrix the estimate of the correction is given by the quantity COFF, defined by

$$\text{COFF} = \tilde{W}'_{n,\max} \int_{R_n}^{R_{n+1}} h_1(R)(R - R_{n+1/2})h_2(R)dR, \tag{25}$$

where $h_1(R)$ and $h_2(R)$ designate either of the linearly independent solutions to Eq. (14) and where $\tilde{W}'_{n,\max}$ designates the largest of the *off-diagonal* elements of the $\tilde{\mathbf{W}}_n'$ matrix. And Gordon has discussed,[18] by symmetry only the $h_1 = h_2$ terms make nonvanishing contributions.

If only the constant term is retained in Eq. (14) then the linearly independent solutions are just trigonometric functions of argument $(\tilde{k}^2_n)^{1/2}_{ii}(R - R_{n+1/2})$.[7,8] In this case one can show, letting k_i denote $(\tilde{k}^2_n)^{1/2}_{ii}$, that

$$\text{COFF} = \frac{\tilde{W}'_{n,\max}}{4k_i^2}\left[\sin k_i\Delta_n - k_i\Delta_n \cos k_i\Delta_n\right], \tag{26}$$

where $\Delta_n = R_{n+1} - R_n$. For $k_i\Delta_n < 1$, this becomes

$$\text{COFF} \simeq k_i\Delta_n^3 \tilde{W}'_{n,\max}/12. \tag{27}$$

It is similarly possible to estimate the correction due to the diagonal elements of the $\tilde{\mathbf{W}}_n''$ matrix. We define

$$\text{CDIAG} = \langle \tilde{W}''_n \rangle \int_{R_n}^{R_{n+1}} h_1(R)(R - R_{n+1/2})^2 h_2(R)dR, \tag{28}$$

where $\langle \tilde{W}''_n \rangle$ designates the average of the magnitudes of the *diagonal* elements of the $\tilde{W}''_n$ matrix. In the case of trigonometric functions we find

$$\text{CDIAG} \simeq \langle \tilde{W}''_n \rangle \Delta_n^3/12. \tag{29}$$

On the basis of this simple reasoning we have decided to use the following equation to predict the interval sizes:

$$\Delta_{n+1} = \Delta_n \left[\frac{\text{TOLHI}}{\max(\langle \tilde{W}''_n \rangle, \bar{k}\tilde{W}'_{n,\max})}\right]^{1/\text{POW}}, \tag{30}$$

where $\bar{k}$ designates the average of the local wave vectors and TOLHI and POW are input parameters. Although Eqs. (27) and (29) suggest that POW should be taken equal to 3, we have found, at least for the numerical example to be discussed in Sec. IV, that slightly improved accuracy can be obtained with POW greater than 3, which reduces the allowed degree of increase in interval size.

The size of the first interval is suggested by Eq. (27). We use

$$\Delta_1 = 0.25\left[12\ \text{TOLHI}/\bar{k}\tilde{W}'_{0,\max}\right]^{1/3}, \tag{31}$$

where $\tilde{W}'_{0,\max}$ designates the maximum off-diagonal element in the transform of the first derivative of the $\mathbf{W}$ matrix at $R = R_{\text{begin}}$. This necessitates one more matrix diagonalization, but this is an insignificant increase in the computational overhead if the total number of intervals N is significantly greater than 1. The factor of 0.25 in Eq. (31) is added to ensure that an error will not be introduced by an overly large choice of the first interval size. A hybrid LOGD/AIRY computer code was written based on the algorithm outlined above. Of the original Gordon code[22] only the subroutines AIRY and SPROP were retained, with the latter modified as described above. All the requisite matrix manipulation subroutines were rewritten to be as simple as possible.

B. VIVS algorithm

In the VIVS algorithm of Parker, Schmalz, and Light[8] the first and second derivative terms are neglected in Eq. (14), so that the reference solutions are trigonometric (or hyperbolic) functions. However, the corrections to all the neglected $\tilde{\mathbf{W}}_n'$ and $\tilde{\mathbf{W}}_n''$ matrix elements are determined as precisely as possible, by further breaking the interval down into a series of smaller steps. An advantage of this approach is that analytic expressions for these correction terms are available for trigonometric reference solutions but not for Airy function reference solutions.[17] The VIVS code propagates the inverse to the local log-derivative matrix, the "sector R matrix",[20] in a manner analogous to Eq. (20). In the calculations reported below the hybrid VIVAS code of Parker *et al.* was used[23,24]; propagation from R_{start} to R_{begin} is achieved with the LOGD algorithm, and from R_{begin} to R_{end} with the VIVS algorithm.

C. Multichannel WKB method

In this method, developed by Johnson,[16] the S matrix is given by

$$\mathbf{S} = \mathbf{G}\tilde{\mathbf{S}}\mathbf{G}^T, \tag{32}$$

where

$$\mathbf{G} = \exp(i\delta)\mathbf{U}(R_{\text{end}}, R_{\text{begin}}), \tag{33}$$

and where δ is a diagonal matrix with elements

$$\delta_i = k_i \int_{R_{\rm end}}^{\infty} \{[1 - l_i(l_i+1)/(k_i R)^2]^{1/2} - 1\} dR - k_i R_{\rm end} + l_i \pi/2. \quad (34)$$

Here the propagation matrix $\mathbf{U}(R_{\rm end}, R_{\rm begin})$ is defined by

$$\mathbf{U}(R_{\rm end}, R_{\rm begin}) = \exp\left[i \int_{R_{\rm begin}}^{R_{\rm end}} \mathbf{K}(R) dR \right], \quad (35)$$

where

$$\mathbf{K}(R) = [\mathbf{W}(R)]^{1/2}. \quad (36)$$

In Eq. (32) the $\tilde{\mathbf{S}}$ matrix is defined by matching the wave function and its derivative at $R = R_{\rm begin}$, obtained by numerical integration from $R_{\rm start}$ to $R_{\rm begin}$, to the form

$$\mathbf{F}(R) = \mathbf{k}^{-1/2} \exp[-i\mathbf{k}(R - R_{\rm begin})] - \mathbf{k}^{-1/2} \times \exp[i\mathbf{k}(R - R_{\rm begin})]\tilde{\mathbf{S}}. \quad (37)$$

It follows from Eqs. (4) and (37) that the $\tilde{\mathbf{S}}$ matrix can be obtained from the numerical value of $\mathbf{Y}(R_{\rm begin})$ by means of the equation

$$\tilde{\mathbf{S}} = (\mathbf{X} - i\mathbf{I})^{-1}(\mathbf{X} + i\mathbf{I}), \quad (38)$$

where

$$\mathbf{X} = \mathbf{k}^{-1/2}\mathbf{Y}(R_{\rm begin})\mathbf{k}^{-1/2}. \quad (39)$$

The propagation matrix is approximated in first Magnus form[18,20]

$$\mathbf{U}(R_{\rm end}, R_{\rm begin}) = \prod_{n=1}^{N} \mathbf{U}_n(R_{n+1}, R_n), \quad (40)$$

where

$$\mathbf{U}_n = \exp\left[i \int_{R_n}^{R_{n+1}} \mathbf{K}(R) dR \right]. \quad (41)$$

In practice the matrix exponentiation is carried out by transformation to a local basis in each interval, exactly as described in Sec. III A above, so that

$$\mathbf{U}_n = \mathbf{T}_n^T \exp[i\Delta_n \tilde{\mathbf{k}}_n] \mathbf{T}_n. \quad (42)$$

If the multichannel WKB method is used to integrate the CC equations in the large-R region, then $R_{\rm begin}$ must be chosen to lie beyond the outermost classical turning point for all the channels retained.

If the $\mathbf{K}$ matrix were diagonal, then the integration in Eq. (35) [or equivalently Eq. (41)] could be done exactly. Thus a crude measure of the error in approximating Eq. (41) by Eq. (42) is given by

$$\mathrm{COFF} = \Delta_n K_{ij}^{\max}(R_{n+1/2}), \quad (43)$$

where $K_{ij}^{\max}(R_{n+1/2})$ designates the largest (in magnitude) *off-diagonal* element of the wave vector matrix at the midpoint of the nth interval. For coupling potentials which vary at long-range as R^{-m} these off-diagonal elements will vary as $R^{-m/2}$. It follows that, to a good approximation, the error can be held constant if the interval sizes are allowed to grow according to the relation

$$\Delta_{n+1} = \Delta_n \left\{ 1 + \frac{\Delta_n}{R_{n+1/2}} \left[1 + \frac{\Delta_n}{R_{n+1/2}} \right]^{m/2} \right\}^{m/2}. \quad (44)$$

The size of the first interval is obtained from the equation

$$\Delta_1 = \mathrm{ERR}[K_{ii}^{\max}(R_{\rm begin})/K_{ij}^{\max}(R_{\rm begin})], \quad (45)$$

where ERR is an input parameter and $K_{ii}^{\max}$ designates the maximum on-diagonal element of the wave vector matrix at $R = R_{\rm begin}$.

The code for this multichannel WKB integrator was adapted from that originally written by Johnson,[19] with successive interval sizes predicted by Eq. (44).

IV. NUMERICAL APPLICATION TO HF–HF COLLISIONS

To ascertain the accuracy and speed of the various hybrid codes, comparison calculations were carried out for a typical long-range system: the collision of two HF molecules at a total energy of 2000 cm^{-1}, which is comparable to the relative translational energy in the ongoing molecular beam experiments of Vohralik and Miller.[25] This energy corresponds to a deBroglie wavelength of $\sim$0.35 bohr. Since it is typically necessary to integrate the CC equations out to a distance of 100–200 bohr to obtain convergence in the S matrix, the need for a fast, accurate large-R integration algorithm is obvious.

The first comparison involved S matrices generated by the various methods for an eight channel basis at a total angular momentum of $J = 100$, equivalent to an impact parameter of 5.5 bohr, which is comparable to the intermolecular distance in the $(HF)_2$ dimer.[26] The channel quantum numbers and internal energies are listed in Table I.

The potential matrix is defined by[19,12]

$$V_{ii}(R) = (4\pi)^{-3/2}(3.05\times10^6\, e^{-2R} - 2.25\times10^4\, e^{-1.1R}) \quad (46)$$

and

$$V_{i,j\neq i}(R) = -(4\pi)^{-3/2} v_{ij}(490e^{-R} + 45e^{-0.475R} + 5233R^{-3}), \quad (47)$$

where the nonzero v_{ij} coefficients are given in Table II. In Eqs. (46) and (47) the energy units are kcal/mol (1 kcal/mol = 1.593 5636$\times10^{-3}$ hartree) and the length units are bohr. The collision reduced mass was taken to be 10.0031 amu. The CC equations for this eight channel basis were integrated from $R_{\rm start} = 4.5$ bohr to $R_{\rm end} = 60.0$ bohr; the classical turning points occur between 5.50 and 5.71 bohr. The value of $R_{\rm begin}$ was taken to be 7.75 bohr.

The accuracy of a particular method was determined by calculation of the root-mean-square (rms) error of both the

TABLE I. HF–HF eight channel basis, $J = 100$, even parity, (+) interchange symmetry.[a]

N	j_1	j_2	j_{12}	l	$\epsilon(\mathrm{cm}^{-1})$[b]
1	0	0	0	100	0.00
2	1	1	0	100	82.222
3	1	1	2	98	82.222
4	1	1	2	100	82.222
5	1	1	2	102	82.222
6	0	2	2	98	123.282
7	0	2	2	100	123.282
8	0	2	2	102	123.282

[a] For details of the formulation of the dynamics and the interpretation of the quantum numbers see Refs. 10–12.
[b] Channel energy.

TABLE II. Nonvanishing coupling coefficients $J = 100$, even parity, (+) interchange symmetry.[a]

i	j	V_{ij}	i	j	v_{ij}	i	j	v_{ij}
1	3	1.362 459 6	2	7	1.000 037 0	4	7	− 0.706 896 66
1	4	− 1.118 075 4	2	8	− 1.230 808 0	4	8	− 0.857 419 06
1	5	1.376 085 2	3	6	0.696 446 81	5	8	0.717 556 56
2	6	− 1.218 620 9	3	7	− 0.874 652 97			

[a] See Eq. (47). Also, $v_{46} = v_{37}$, $v_{57} = v_{48}$; all other v_{ij} are identically zero.

elastic, and separately, the inelastic S-matrix elements, namely

$$\Delta^2_{\rm rms} = \sum_{i=1}^{M} \left\{ \frac{1}{M}[R_e(\bar{S}_i) - R_e(S_i)]^2 + \frac{1}{M}[I_m(\bar{S}_i) - I_m(S_i)]^2 \right\}, \quad (48)$$

where $M = 8$ for the elastic comparison and $M = 28$ for the inelastic comparison. Here S_i denotes an "exact" S-matrix element and $\bar{S}_i$ denotes the value determined by the particular calculation in question. The exact S-matrix elements were determined by a LOGD calculation from 4.5 to 60 bohr with an interval size of 0.005 bohr. These values are available on request.

Figure 1 displays the rms error in the elastic and inelastic S-matrix elements as a function of CPU time required by each hybrid code for the integration from $R_{\rm begin} = 7.75$ bohr to $R_{\rm end} = 60.0$ bohr. The various entries correspond to different choices of the input tolerance parameters. For the AIRY integrator as described in Sec. III we chose POW = 5 in Eq. (30) and used values of TOLHI ranging from 0.003 to 40. For the VIVS integrator we used the input parameters[23] DRNOW = 0.1, IALPHA = 6 (corresponding to six steps/interval), and values of the tolerance parameter[23] TOFF ranging from 0.001 to 1. For the WKB integrator the values

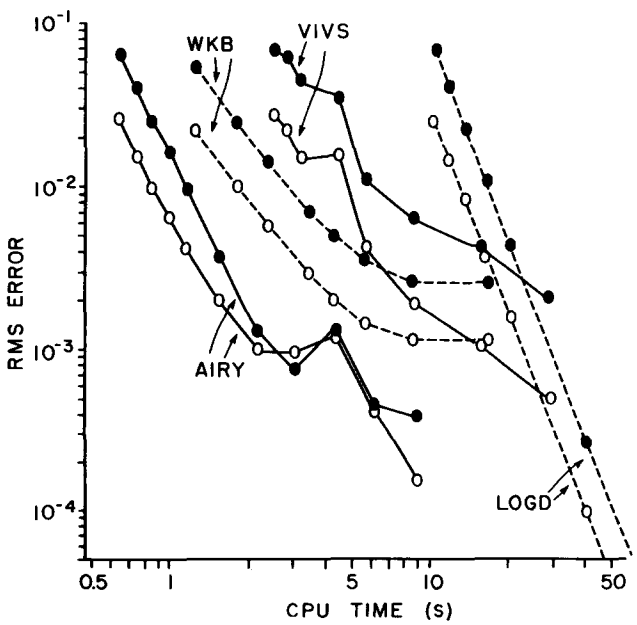

FIG. 1. Root-mean-square error in both elastic (filled circles) and inelastic (open circles) S-matrix elements [Eq. (48)] as a function of CPU time (UNIVAC 1100/82) for integration of eight channel HF–HF problem from $R = 7.75$ to $R = 60.0$ bohr. For clarity the WKB and LOGD results are connected by dashed lines; and the AIRY and VIVS results, by solid lines.

of the tolerance parameter ERR in Sec. IV ranged from 0.003 to 0.1. For comparison, we also display curves corresponding to a pure LOGD integration from 4.5 to 60.0 bohr with step sizes ranging from 0.0075 to 0.04 bohr. The CPU times refer to the UNIVAC 1100/82 at the University of Maryland with the FTN compiler without optimization.

We make the following observations: First, the LOGD algorithm appears to be a *higher order* method[3,18] than the other three, in that the accuracy of the computed S matrix converges as a higher inverse power of the CPU time. Secondly, the convergence is nonmonotonic in the case of both the AIRY and, more markedly, VIVS integrators. Thirdly, in the case of the WKB algorithm there appears to be a maximum achievable accuracy, which probably reflects the inherent error in the WKB approximation to the true wave function, which would subsist even if the propagation matrix [Eq. (35)] were determined precisely. This inherent inaccuracy appears to be sensitive to the choice of $R_{\rm begin}$; when the latter is reduced to 6.75 bohr, the maximum attainable accuracy in the elastic S-matrix elements drops to $\sim 2 \times 10^{-2}$. Only one set of curves for the VIVS integrator is displayed. Variation of the input tolerance parameters DRNOW and IALPHA, which control the initial step size and the number of steps per interval, did not significantly improve either the accuracy or convergence of the calculated S matrix.

In the eight channel comparison summarized in Fig. 1 the AIRY integrator is obviously the fastest. To assess the relative speeds for larger bases we have carried out additional calculations for 17, 33, and 49 channels, which correspond to full CC calculations on the HF–HF system identical to those described above, except that the rotational basis was extended as summarized in Table III. In each case the value of $R_{\rm begin}$ was taken to be 7.75 bohr but the value of $R_{\rm end}$ was extended to 90 bohr. (In fact it is necessary to take $R_{\rm end} > 150$ bohr to obtain full convergence of the S matrix for this particular problem; however, a value of $R_{\rm end} = 90$ bohr is sufficiently large to discriminate among the various integrators). In each case the relevant tolerance parameters were chosen to ensure an accuracy of 0.01 in the elastic S-matrix elements. We were guided by the convergence study illustrated in Fig. 1. The particular values of these tolerance parameters, as well as the actual CPU time for these larger channel calculations, are listed in Table IV.

We observe that regardless of the number of channels the AIRY integrator is nearly 20 times faster than the LOGD integrator, for the medium-to-large R region. As is well known,[3,8,17,18] any potential-following method is much more efficient for calculations at a second energy, where the interval sizes and transformation matrices [Eq. (22)] deter-

TABLE III. HF–HF rotational states included in scattering calculations; $E = 2000\ \text{cm}^{-1}$, $J = 100$, even parity, $(+)$ exchange symmetry.[a]

N_{ch}[b]	Rotational states included[a]
8	00,11,02
17	00,11,02,22
33	00,11,02,22,13,04
49	00,11,02,22,13,04,33

[a] For details of the formulation of the dynamics and the description of the channel bases, see Refs. 10 and 12.
[b] Total number of coupled channels.

mined for the first energy can be used without change. The AIRY integrator described here is approximately *three times faster at a second energy*, as seen in the CPU times listed in Table IV.

The multichannel WKB integrator is approximately three times slower than the AIRY integrator, irrespective of the number of channels. In each case the WKB integrator required ~ 75 intervals, whereas the AIRY integrator required 26 intervals. Thus the two integrators are seen to be equally fast *per interval*, so that it might be possible to accelerate the WKB integrator by permitting the interval size to increase faster than allowed by Eq. (44), provided, of course, that this did not compromise the accuracy.

We observe in Table IV that the VIVS integrator becomes somewhat more competitive as the number of channels increases. The VIVS integrator required ~ 25 intervals with the choice of tolerance parameters listed in Table IV. In the limit of an infinitely large number of channels, where the required CPU time will be dominated completely by matrix operations, the VIVS integrator should become increasingly competitive relative to the AIRY integrator, since both require essentially the same matrix transformations. However, we anticipate that even in this limit the AIRY integrator, which required 26 intervals, will be faster, since the symmetry of the log-derivative matrix, which is lost when first-order corrections are included, reduces the operation count for the transformations associated with Eqs. (20) and (23).

It is perhaps surprising that the AIRY integrator appears to be so much more efficient than the VIVS integrator,

TABLE IV. CPU time in seconds required to integrate from $R_{begin} = 7.75$ bohr to $R_{end} = 90$ bohr, as a function of the number of channels.[a]

Integrator	17 ch	33 ch	49 ch
AIRY (second)[b]	2.7	17.3	54.3
AIRY (first)	8.5	53.5	163
WKB	24.4	161	516
VIVS	64.6	281	857
LOGD	151	988	3150

[a] CPU time on UNIVAC 1100/82. Input parameters were estimated from Fig. 1 to ensure an accuracy of 1×10^{-2} in the elastic S-matrix elements. Specific values were, for the AIRY algorithm, POW = 5 and TOLHI = 3; for the WKB algorithm, ERR = 0.66; for the VIVAS algorihm (Ref. 23), DRNOW = 0.1, IALPHA = 6, TOFF = 0.01; and for the LOGD algorithm, a step size of 0.025 bohr.
[b] CPU time for calculation at a second energy, where the previously determined $\mathbf{P}_n$ transformation matrices [Eq. (22)] can be read in from disk.

at least for the R^{-3} system studied here. During the NRCC workshop on molecular scattering codes, in test calculations on a system with an R^{-2} coupling potential the VIVS integrator was found[4] to be ~ 4 times faster than the Gordon integrator, which is based on an Airy function propagation algorithm. The speed of the present AIRY integrator, when compared to the VIVS and Gordon codes, arises primarily from the elimination of the calculation of all corrections due to the neglected terms of the $\tilde{\mathbf{W}}_n'$ and $\tilde{\mathbf{W}}_n''$ matrices. As illustrated by Fig. 1, determination of these correction terms is not necessary, at least in the present application.

An additional advantage of the AIRY code lies in the size of the object code and matrix storage requirements. The object code for the hybrid LOGD/AIRY integrator occupied 10 000 36 bit words on a UNIVAC 1100/82 computer (FTN compiler), with an additional $6.5M^2$ words of storage (M being the number of channels) for the various matrices needed during the integration of the CC equations. By contrast the VIVAS code occupied 15 000 words with an additional $11M^2$ words of matrix storage. The reduced size of the LOGD/AIRY integrator could be a significant advantage in a multitask environment or whenever the charging algorithm is dependent on core use as well as execution time.

Finally, as discussed in Sec. III A, the matrix manipulation routines used in the LOGD/AIRY integrator have been drastically simplified over those appearing in the original Gordon code,[22] which contained sophisticated procedures designed to deal with ill-conditioned matrices. As evidenced by the high accuracy of Johnson's original LOGD code,[4,19] which incorporates extremely simple matrix manipulation routines, the matrices which characterize typical molecular close-coupling calculations are well behaved.

V. CONCLUSION

We have investigated hybrid codes for molecular scattering calculations which combine the log-derivative (LOGD) integrator of Johnson[6,19] for short interparticle separations with one of the three following integrators for moderate to large interparticle separations: (1) the multichannel WKB algorithm of Johnson[16]; (2) the variable-interval-variable-step (VIVS) algorithm of Parker, Schmalz, and Light[8]; and (3) a locally adiabatic Airy function algorithm (AIRY) based on the original algorithm of Gordon,[17,18] but modified to propagate the log-derivative matrix directly without determination of any perturbation corrections. In calculations of S matrices for the collision of two HF molecules, a typical long-range system, the hybrid code based on the AIRY intergrator proved to be considerably faster than the codes based on the WKB or VIVS integrator. In the case of the WKB integrator the speed advantage was a factor of ~ 3, independent of the number of channels, and, in the case of the VIVS integrator, the speed advantage was 7.6, 5.3, and 5.3 for 17, 33, and 49 channel calculations, respectively. Furthermore, the AIRY integrator is approximately 19 times as fast as the LOGD integrator in the long range region.

Obviously, then, a hybrid LOGD/AIRY integrator appears to be the algorithm of choice for scattering calculations involving long-range coupling potentials, in terms of speed, accuracy, and compactness of code. Additional studies indi-

cate that even for primarily repulsive potentials the LOGD/AIRY hybrid code runs substantially faster than the pure LOGD code. Further improvements are certainly possible, particularly in the step size algorithm, and should be the object of future research.

ACKNOWLEDGMENT

The research described here was supported in part by the National Science Foundation, grant CHE81-08464 and by the Computer Science Center, University of Maryland. The author is grateful to Tadeusz Orlikowski for his help in adapting the original VIVAS code, generously supplied by Gregory Parker, to treat the collision of two HF molecules.

[1]For an excellent review, see D. Secrest, in *Atom–Molecule Collision Theory: A Guide for the Experimentalist*, edited by R. B. Bernstein (Plenum, New York, 1979), p. 265.
[2]L. D. Thomas, M. H. Alexander, B. R. Johnson, W. A. Lester, Jr., J. C. Light, K. D. McLenithan, G. A. Parker, M. J. Redmon, T. G. Schmalz, D. Secrest, and R. B. Walker, J. Comput. Phys. **41**, 407 (1981).
[3]*Proceedings of the NRCC Workshop on Algorithms and Computer Codes in Atomic and Molecular Scattering Theory*, edited by L. D. Thomas, Lawrence Berkeley Laboratory Report LBL-9501 (Lawrence Berkeley, Berkeley, CA, 1979), Vol. I.
[4]*Proceedings of the NRCC Workshop on Algorithms and Computer Codes in Atomic and Molecular Scattering Theory*, edited by L. D. Thomas, (Lawrence Berkeley Laboratory Report LBL-9501 (Lawrence Berkeley, Berkeley, CA, 1980), Vol. II.
[5]See B. R. Johnson, pp. 86–92 of Ref. 3 and p. 52 of Ref. 4.
[6]B. R. Johnson, J. Comput. Phys. **13**, 445 (1973).
[7]F. Mrugala and D. Secrest, J. Chem. Phys. **78**, 5954 (1983).
[8]G. A. Parker, T. G. Schmalz, and J. C. Light, J. Chem. Phys. **73**, 1757 (1980).
[9]G. A. Parker, J. C. Light, and B. R. Johnson, Chem. Phys. Lett. **73**, 572 (1980).
[10]A. E. DePristo and M. H. Alexander, J. Chem. Phys. **66**, 1334 (1977).
[11]M. H. Alexander and A. E. DePristo, J. Chem. Phys. **66**, 2166 (1977).
[12]M. H. Alexander, J. Chem. Phys. **73**, 5135 (1980).
[13]S. Bosanac, J. T. Brobjer, and J. N. Murrell, Mol. Phys. **51**, 313 (1984).
[14]E. M. Lifshitz, Sov. Phys. JETP **2**, 73 (1956); W. A. Steele, *The Interaction of Gases with Solid Surfaces* (Pergamon, Oxford, 1974).
[15]See, for example, J. E. Hurst, Jr., G. D. Kubiak, and R. N. Zare, Chem. Phys. Lett. **93**, 235 (1982); J. M. Hutson and C. Schwartz, J. Chem. Phys. **79**, 5179 (1983).
[16]B. R. Johnson, Chem. Phys. **2**, 381 (1973).
[17]R. G. Gordon, J. Chem. Phys. **51**, 14 (1969).
[18]R. G. Gordon, Meth. Comput. Phys. **10**, 81 (1971).
[19]Program KQ06 (LOGD), available from Quantum Chemistry program Exchange, Department of Chemistry, Indiana University, Bloomington, IN 47405.
[20]E. B. Stechel, R. B. Walker, and J. C. Light, J. Chem. Phys. **69**, 3518 (1978).
[21]Equation (23) is equivalent to Eq. (13) of Ref. 8, which describes the transformation of the R matrix from one interval to the next.
[22]Program 187 (QCOL), available from Quantum Chemistry Program Exchange, Department of Chemistry, Indiana University, Bloomington, IN 47405.
[23]Program KQ04 (VIVAS), available from Quantum Chemistry Program Exchange, Department of Chemistry, Indiana University, Bloomington, IN 47405.
[24]The calculations described in Sec. IV involved a modified code (VIVAS-II), generously supplied by G. A. Parker, Department of Physics, University of Oklahoma, Norman, OK 73069.
[25]P. F. Vohralik and R. E. Miller, J. Chem. Phys. (submitted).
[26]M. H. Alexander and A. E. DePristo, J. Chem. Phys. **65**, 5009 (1976); J. T. Brobjer and J. N. Murrell, Mol. Phys. **50**, 885 (1983).